Agronomy Research **23**(X), xxx–ccc, 2025
https://doi.org/10.15159/AR.25.051

Assessment of CO_2 emission rate from extended area sources with WindTrax model in a dairy cattle farm

A. Mattia, M. Merlini, F. Squillace, G. Rossi, L. Conti and V. Becciolini*

University of Florence, Department of Agriculture, Food, Environment and Forestry, via San Bonaventura 13, IT 50145 Firenze, Italy
*Correspondence: valentina.becciolini@unifi.it

Received: February 14th, 2025; Accepted: May 26th, 2025; Published: June 19th, 2025

Abstract. This paper aimed to evaluate the WindTrax model to quantify CO_2 (carbon dioxide) emissions in a commercial dairy cattle farm in Central Italy with a low-cost measurement system. A field trial of 20 minutes was conducted in February 2023, using two G-eko 2.0 MSPs (multi-sensor platforms), an anemometer, and a GNSS receiver, in unstable atmospheric conditions. Then, 5-minute averaged data were used as input in the WindTrax software for applying the backward Lagrangian Stochastic model. The model was used for calculating four mean CO_2 emission rates (0.20212 ± 0.04994 g m^{-2} s^{-1}) with 50,000 particles and the horizontal dispersion of CO_2 concentrations around the sources using different numbers of particles (5,000, 10,000, 30,0000, and 50,000). Atmospheric dispersion maps, confidence interval concentration maps, and vertical profile plots were obtained by increasing the number of particles. The model shows better performances, in terms of confidence intervals, with a high number of particles with a stabilization of modeled median values between 30,000 and 50,000 particles. Horizontally, the lowest confidence intervals (near to zero) were obtained at 100–150 m from the sources along the wind direction, suggesting that the downwind sensor could be placed at a greater distance. Similarly, a better-defined vertical trend in modeled concentrations is observed as the number of particles increases. Wind gusts could have a great effect on emission rate calculation with limited sampling periods, as in this case, but simultaneously unstable atmospheric conditions affect the increased dispersion and dilution of CO_2.

Key words: greenhouse gases, livestock farming, low-cost sensors, pollutants dispersion.

INTRODUCTION

In recent decades, the exponential increase in human activities has significantly intensified the anthropogenic greenhouse effect, resulting in rising global temperatures and, consequently, climate change. This has increased public awareness of pollution and environmental issues (Tagliaferri et al., 2020). According to the IPCC (2022) report on global emission data from 2015, the livestock sector accounted for 12–17% of total greenhouse gases (GHGs) emissions, with cattle farming contributing 62% of the sector's total emissions (Global Livestock Environmental Assessment Model 3

dashboard, 2022). Within livestock farms, the primary sources of emissions are enteric fermentation in ruminants (67–68%), manure and slurry storage (23–26%), and feed production (Ripple et al., 2014; Grossi et al., 2019).

Environmental chemical monitoring is essential in bottom-up approaches for emissions inventories and for identifying critical processes that could benefit from targeted mitigation strategies. Various gas sensor technologies are available for this purpose, including amperometric gas sensors (AGS), metal oxide semiconductor sensors (MOX or MOS), nondispersive infrared sensors (NDIR), and photoionization detectors (PIDs) (Cambra-López et al., 2010; Burgués & Marco, 2020). To improve monitoring efficiency, multi-sensor platforms (MSPs) have been developed, enabling the simultaneous operation of multiple sensors. These platforms facilitate the collection of gas concentration data alongside meteorological parameters, providing a comprehensive assessment of emissions (Burgués et al., 2018).

Currently, monitoring GHG emissions is expensive due to the cost of accurate sensors in the market, but the ongoing technological development provides low-cost sensors. The objective of this study was to assess CO_2 emissions obtained with self-engineered multi-sensor platforms on a dairy farm, through the estimation of emission fluxes and the graphical representation of gas concentrations and concentration confidence intervals across the farm area. By employing the WindTrax model to simulate the horizontal and vertical dispersion of the target gas, farmers could adopt an accurate low-cost measurement system that works autonomously, aiming to provide management insights. WindTrax is widely used in agrometeorological studies to estimate emission rates, particularly for GHGs and ammonia (Lin et al., 2015; Yang et al. 2016; Hrad et al., 2021; Genedy & Ogejo, 2022). Existing research primarily evaluates its accuracy in modeling pollutant emissions from area sources, highlighting its relevance as a tool for emission assessment and atmospheric dispersion analysis. Thus, an affordable and accurate emission measurement system that can be easily implemented on commercial farms is needed by farmers to identify critical emission sources, adopting appropriate mitigation strategies.

This study investigated the impact of livestock-related activities on GHG emissions, with a focus on data analysis through specialized simulation methodologies. Specifically, CO_2 (carbon dioxide) emissions were examined using low-cost sensing platforms and atmospheric dispersion modeling as tools for rapid on-farm assessment. This study represented the first application of low-cost sensing platforms combined with dispersion modelling to assess gas emissions and dispersion from livestock buildings in the study area. The study was conducted as part of a research project aiming at assessing greenhouse gases emissions from dairy cattle and swine farming systems across Northern, Central, and Southern Italy using innovative measurement techniques. In Central Italy, the Tuscany region ranks second in terms of dairy cattle population (data provided by the National Zootechnical Registry -BDN- of the Italian Ministry of Health, managed by the 'G. Caporale' Institute in Teramo through the National Services Centre -CSN-). One of the two main dairy production districts in Tuscany is located in the Province of Florence, specifically in the Mugello area, which hosts both larger farms (over 200 lactating cows) and medium-sized farms.

MATERIALS AND METHODS

Study site

The experiment was conducted on a commercial dairy farm in the Mugello area, Province of Florence (Central Italy). The selected farm is representative of the medium-sized dairy farms commonly found in this region. The farm primarily focused on dairy cattle breeding but also operated as an educational farm and agritourism. The cattle housing facility was open on all four sides, and it was situated on relatively flat terrain. At the time of the experiment, the farm housed 123 Holstein Friesian dairy cows in the main building for milk production. Of these, 65 lactating cows were kept in a free-stall pen with cubicles in the resting area and straw bedding, while the remaining 58 cows and heifers were housed in deep-litter pens with permanent straw bedding. All pens had concrete-floored feeding alleys and were equipped with water troughs. A Total Mixed Ration (TMR) was distributed once daily at h 18 00, and a robotic feed pusher regularly repositioned the feed along the self-locking headlocks.

Additionally, 12 calves were kept in individual pens adjacent to the stable, and 12 Belgian Blue White fattening cattle were also present in a pen in the south-east part of the stable. The farm also accommodated a chicken coop and a few donkeys. Contributions to the total emissions were considered negligible.

The slurry from the two rows of pens inside the livestock building, one with permanent litter and the other in cubicles with straw bedding, was collected by automatic scrapers into two underground concrete tanks. The solid fraction, separated from the liquid, was stockpiled in a rectangular uncovered pit. In contrast, the liquid fraction was transferred to an open-air, circular underground concrete tank located north of the stable (Fig. 1).

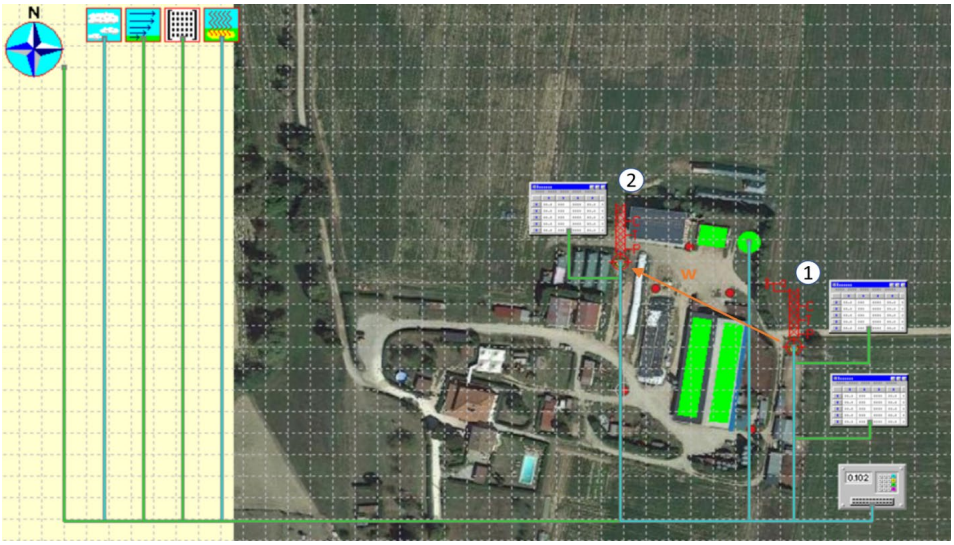

Figure 1. View of the commercial dairy farm (latitude 43.963270°, longitude 11.418885°) and inside the project of the WindTrax software environment. Point 1: upwind G-eko 2.0 multi-sensor unit. Point 2: downwind G-eko 2.0 multi-sensor unit.

Instrumentation

A dual-frequency GNSS receiver (GCX2, Sokkia, Netherlands) with centimetric accuracy was used to georeference the measurement points. Gas concentrations and microclimate parameters were measured using the G-eko 2.0, a self-engineered multi-sensor prototype described in Becciolini et al. (2023). The module, measuring 120×100×67 mm and weighing 0.75 kg, was designed for environmental monitoring. G-eko 2.0 included sensors for measuring CO_2, NH_3, CH_4, $PM_{2.5}$ and PM_{10} together with atmospheric pressure, temperature, and humidity.

CO_2 was measured using a Non-Dispersive InfraRed (NDIR) sensor, which also integrated temperature and humidity sensors within the same module. The CO_2/T/RH module had dimensions of 23×35×7 mm and a weight of 3.4 g. The technical specifications of the sensing module are detailed in Table 1.

Table 1. Specifications of the cmOSens sensing module

Target parameter	Measurement unit	Measuring range	Accuracy
CO_2	ppm	0 ÷ 5,000	± 30
Temperature	Celsius degree	–40 ÷ +70	± (0.4 + 0.023 (T – 25))
Relative humidity	%	0 ÷ 100	± 2

The NDIR sensor was selected due to its documented suitability for CO_2 measurements, attributed to its strong and distinct absorption peak in the mid-infrared region, and the absence of common limitations associated with low-cost electrochemical sensors, such as inter-device variability and susceptibility to poisoning by silicone vapours (Burgués & Marco, 2020). Given the documented influence of temperature on the accuracy of NDIR sensors (Martin et al. 2017), the sensor integrated into the first prototype of the multi-sensor system (G-eko 1.0) was calibrated by an independent laboratory under controlled temperature and humidity conditions (Becciolini et al., 2024a). To improve environments, an additional calibration was conducted on the G-eko 2.0 prototype under different temperature and humidity regimes, enabling the development of correction equations applicable to diverse environmental conditions (Becciolini et al., 2024b).

The anemometer (WT87B, Shenzhen Wintact Electronics Co., Ltd., China) used in this study is shown in Fig. 2. This device measured wind speed, temperature and humidity.

Through a dedicated mobile application, the sensor can connect to a smartphone, enabling real-time data recording and storage. The technical specifications of the sensor are provided in Table 2.

Figure 2. Anemometer (WT87B, Shenzhen Wintact Electronics Co., Ltd., China).

Table 2. Specifications of the WT87B anemometer

Target parameter	Measurement unit	Measuring range	Accuracy	Resolution
Wind speed	m s^{-1}	0 ÷ 30	± 5% ±0.1	0.01
Temperature	Celsius degree	-10 ÷ +45	± 2	0.1
Relative humidity	%	10 ÷ 90	± 5	0.1

Software

Two software packages were used for the analyses: WindTrax (version 2.0.9.7, Thunder Beach Scientific) and QGIS (3.22.5 version, QGIS.org, 2023, QGIS Geographic Information System. QGIS Association. http://www.qgis.org).

WindTrax incorporates the WindTrax atmospheric dispersion model (Flesh & Wilson, 2005) and is designed to simulate the dispersion of target gases from both point and extended area emission sources. It includes three modeling approaches: the Atmospheric Surface Layer model, the forward Lagrangian Stochastic (fLS) model, and the backward Lagrangian Stochastic (bLS) model. The bLS model is suited for extended area sources and was used in this study to estimate the CO_2 emission rate (Q, g m^{-2} s^{-1}) from various sources, including two rows of pens in the main building, the manure storage, and the slurry storage tank located north of the livestock building (Fig. 1). To run the bLS model, WindTrax requires four parameters describing the surface layer wind model: surface roughness length (z_0, cm), friction velocity (u_*, m s^{-1}), atmospheric stability or Monin-Obukhov length (L, m), and mean horizontal wind direction (θ, degrees) (Crenna, 2006a). Additionally, at least one gas concentration measurement per source is needed to estimate the unknown emission rates (Flesch et al., 1995). The model also requires a background concentration (C_{BG}), which can be entered directly if known or derived from an upwind concentration measurement. The software then solves a system of equations to calculate coefficients that relate emission rates to measured concentrations and vice versa (Crenna 2006a; Crenna 2006b).

QGIS, an open-source geographic information system (GIS) software, was used both before and after WindTrax simulations. Initially, it was employed to georeference the two sampling points and generate a scaled map for exporting into WindTrax (Fig. 1), ensuring accurate distance proportions within the software. After the simulations, QGIS was used to create raster images visualizing the atmospheric dispersion of CO_2 as modelled by WindTrax.

Experimental setup

The experiment was conducted during a single day in February 2023. First, the prevailing wind direction was determined. Two G-eko 2.0 units were then positioned at the height of 1 m from the ground, one upwind (sampling point 1) and one downwind (sampling point 2) of the emission sources (Fig. 1), aligned with the wind direction. The units were positioned away from obstacles (Flesch & Wilson, 2005; Crenna et al., 2008). The anemometer was placed upwind, near the G-eko 2.0 unit, at a height of 2 m above the ground. Both G-eko 2.0 units recorded CO_2 concentrations (ppm), atmospheric pressure (Pa), and temperature (°C) at a sampling rate of 5 seconds. Wind speed (m s^{-1}) was measured at a sampling rate of 1 second, while wind direction was estimated. Data collection was conducted continuously for 20 minutes. The choice of the sampling period is due to the fact that the 15-minute averaging period is the most commonly used to include homogeneous weather conditions in the analysis, as suggested by the software author (Crenna, 2006b) for capturing representative atmospheric conditions. Furthermore, this work was part of a larger field trial involving measurements at different heights above the ground, so only this data on a 20-minute sampling period was available. Another reason to choose a 20-minute sampling period is the variability of the wind direction, estimated during the field trial and considered with a constant value during the field trial.

Data processing

After the field trial, data were exported in .csv format. A verification process was conducted to ensure data quality, which included assessing whether the recorded values fell within expected ranges and evaluating the consistency between measurements obtained from the two G-eko 2.0 units.

All collected data were processed using Microsoft Excel to generate input files for WindTrax simulations. The following data processing description has not previously been applied, primarily due to the short duration of the field trial, which imposed specific methodological constraints. Other authors (Lin et al., 2015; Pedone et al., 2017) used data obtained by field trials of longer duration, so the sampling period suggested by the author of the software (Crenna, 2006b) was used. Measurements from the G-eko 2.0 units were averaged at 1-minute intervals, resulting in two datasets of 20 values. The same procedure was applied to wind data yielding, in total, three datasets of 20 measurements each. The scaled map of the farm, created in QGIS, was imported into WindTrax to design the extended area sources and accurately locate the sampling points used during the field trial (Fig. 1). The area sources are represented in lime green and the orange arrow represents wind direction. WindTrax requires the specification of sampling points locations and corresponding datasets; therefore, each point was linked to the corresponding dataset (Fig. 1).

Each set of paired measurements of CO_2 concentration collected upwind (C1, N 20) and downwind (C2, N = 20), along with wind data (N = 20) was entered into the model to generate 20 simulations, each estimating an emission rate (Q, g m^{-2} s^{-1}). Regarding model specifications, the surface roughness length (z_0) was set to 2.3 to represent the short grass surrounding the livestock farm, which is bordered by arable land. The friction velocity u_* was calculated by the model based on wind speed measurements recorded by the anemometer during the field trial. Atmospheric stability was classified as B according to the Pasquill-Gifford stability classes considering wind speeds below 2 m s^{-1} and weak daytime solar radiation. The mean horizontal wind direction (θ) was determined using topographic methods based on GPS coordinates of the two sampling points aligned with the wind direction during the field trial, yielding a value of approximately 119.3°. The number of particles in the simulation was set to 50,000.

The 20 calculated Q values were converted into a dataset obtained by averaging the collected data over 5-minute intervals. These data were used to run additional 16 simulations to model CO_2 dispersion over a 270 m × 230 m area. The area was defined based on emission sources and wind direction to represent CO_2 concentrations at a height of 2 m above the ground. The simulation parameters remained the same as previously stated, and the number of particles was set to 5,000 (N = 4 simulations), 10,000 (N = 4), 30,000 (N = 4), and 50,000 (N = 4). Each simulation generated a raster image consisting of 10,000 pixels, with each pixel representing an estimated CO_2 concentration (ppm). These raster images were georeferenced in QGIS by constructing a rectangle of matching dimensions. This kind of analysis was not used by any of the authors of the analysed literature, but it helps to make the measuring system reliable. The method of implementation for obtaining atmospheric dispersions was, however, in accordance with the software manual (Crenna 2006a; Crenna 2006b).

A similar approach was applied to the calculation of vertical profile plots at the sampling point 2. Using the calculated Q values, 16 vertical profile plots of estimated

CO_2 concentrations were modelled. The simulation parameters were the same as those used for the CO_2 dispersion model. Each vertical profile plot provided estimated CO_2 concentrations at heights ranging from 1 to 10 m above the ground, at an interval of 1 m. Both the CO_2 horizontal dispersion and vertical profile estimates were generated along with their respective confidence intervals. R (R Core Team, 2024, version 4.4.0) and Rstudio (Rstudio Team, 2024, version 2024.4.1.748) were used for data analysis by selecting the library function ggplot2 (Wickham, 2016) for creating the vertical profile plots.

RESULTS AND DISCUSSION

The input data were averaged over five minutes and subsequently used for the WindTrax simulations. This averaging period was selected because of the short sampling period adopted during the field trial, despite WindTrax's potential sensitivity to short-term wind speed and direction variability. Table 3 shows measurements obtained from the G-eko 2.0 units at sampling point 1 (upwind) and 2 (downwind), and the anemometer, which were employed to calculate CO_2 emission rates (Table 4). The highest CO_2 emission rate was obtained for the fourth step, which corresponds to the period with the maximum detected wind speeds.

Table 3. Input data averaged over five minutes detected by the two G-eko 2.0 units and the anemometer at the sampling point 1 (upwind) and 2 (downwind)

Step (run nr.)	Time (CET)	Upwind sampling point					Downwind sampling point		
		temp. (°C)	atm. pressure (Pa)	CO_2 (ppm)	wind speed (m s^{-1})	wind direction (°)	temp. (°C)	atm. pressure (Pa)	CO_2 (ppm)
1	10:40	10.47	99,568	450.14	0.73	119.3	9.59	99,636	637.68
2	10:45	10.55	99,561	453.98	0.72	119.3	9.47	99,630	635.83
3	10:50	10.39	99,555	448.51	0.57	119.3	9.43	99,627	629.10
4	10:55	10.43	99,557	442.26	1.04	119.3	9.58	99,624	621.08

It should be considered that for all the four steps the atmospheric stability was considered class B (unstable), hence the simulations calculating emission rates are influenced by the wind gusts. For example, observing Tables 3 and 4, step 4 is characterised by maximum wind speed and a consequent calculation of a notable peak in CO_2 emission rate, compared to the other steps. In order to understand the influence of the wind on measured concentrations, i.e. whether the values of detected concentration depends on a real increase of emission rates or on increased particle transport due to increased wind speed, a recent study (Mousavi et al., 2025) assessed the influence of meteorological variables on measured CO_2 concentrations in the Middle East. The correlation between wind speed and CO_2 concentrations is inverse significantly in colder months. The paper explains that higher wind speeds lead to a

Table 4. CO_2 emission rates averaged over five minutes calculated using the WindTrax model (50,000 particles)

Step (run nr.)	Time (CET)	Q (g m^{-2} s^{-1})
1	10:40	0.19902
2	10:45	0.19054
3	10:50	0.14932
4	10:55	0.26958

reduction in detected concentrations through the dispersion and dilution processes. Consistently, in this case, the maximum detected concentrations are not reached upwind and downwind with the maximum wind speed (Table 4), thus it is possible to state a greater dispersion of CO_2 at higher wind speeds. In this study, input data were averaged over 5 minutes and not over an interval of 15–30, as recommended by the author of the software. Shorter averaging periods are more subject to wind gusts and in conditions of atmospheric instability, indeed some studies (Carozzi et a., 2013; Tagliaferri et al., 2023) have highlighted a worse level of accuracy in the calculation of emission rates, underestimating them.

Simulations were conducted for all the four steps, covering the entire sampling period. Different numbers of particles (5,000, 10,000, 30,000, and 50,000) were tested, yielding various outputs including concentration maps, confidence interval maps, and vertical profile plots.

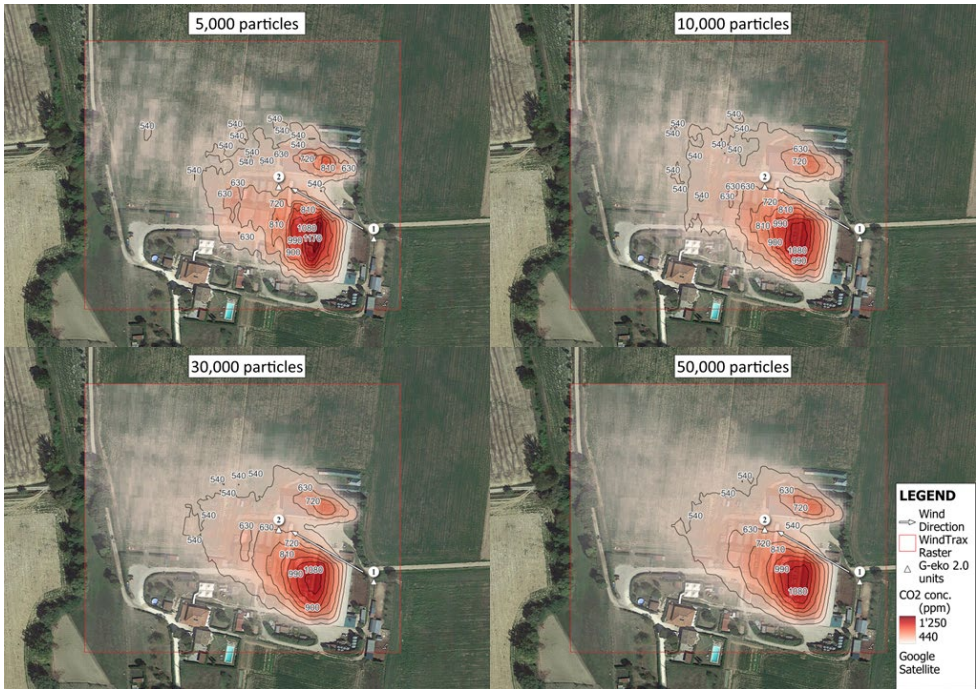

Figure 3. Concentration maps for estimated CO_2 horizontal dispersion at 2 m above ground level modeled with WindTrax simulations using CO_2 measurements averaged at 5-minute intervals. From top left, horizontal contour plots (10 classes separated by 90-ppm intervals) for models computed with 5,000, 10,000, 30,000, and 50,000 particles.

The concentration maps in Fig. 3 were generated for step nr. 1 using different numbers of particles, and indicate the simulated CO_2 concentrations at the height of 2 m above the ground. A uniform colour scale was applied to all four concentration maps, using ten value classes ranging from a minimum of 440 ppm to a maximum of 1,250 ppm, with intervals of 90 ppm, to create horizontal contour plots. Additionally, Fig. 4 shows the concentration map generated for step nr. 1 using 50,000 particles at the height of 2 m above the ground, also representing the emission sources.

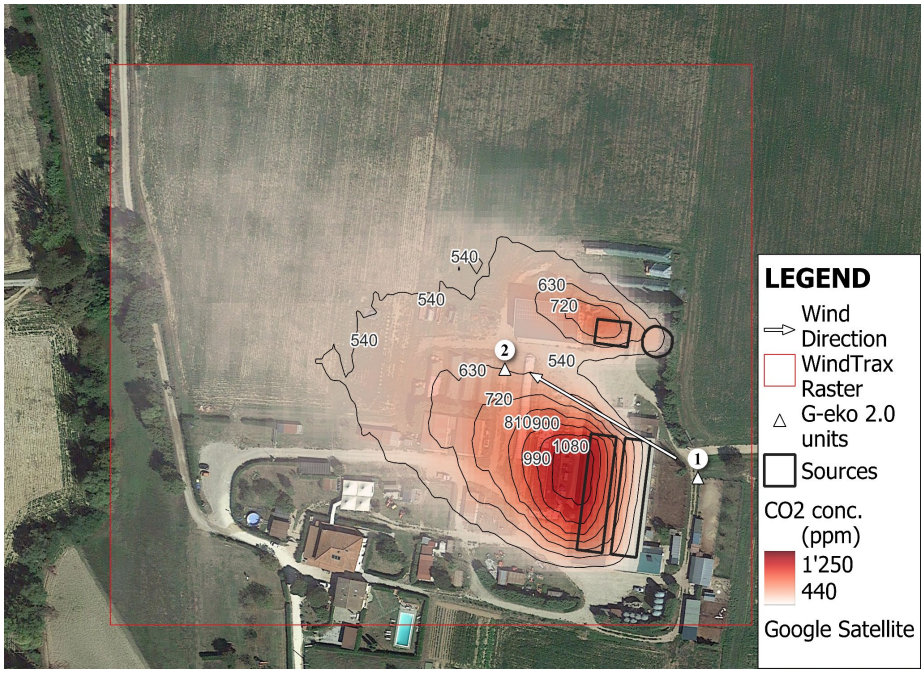

Figure 4. Concentration maps for estimated CO_2 horizontal dispersion at 2 m above ground level modeled with WindTrax simulations using CO_2 measurements averaged at 5-minute intervals. Horizontal contour plots (10 classes separated by 90-ppm intervals) for models computed with 50,000 particles. The sources are shown, as well.

Table 5 shows the results of the concentration maps corresponding to the four steps in terms of maximum and minimum values of the 10,000 estimated concentrations, while Fig. 5 shows the results of the concentration maps corresponding to the four steps in terms of median values. The median was selected to summarize the distribution due to the high number of minimum concentration values located in the periphery of the raster files for each step. Reporting mean values with standard deviation would have provided a misleading interpretation of the results of the simulations. A general trend was noted across all the steps: the median concentration values tend to stabilise with a high number of particles (30,000 and 50,000).

Table 5. Simulated CO_2 concentrations (maximum and minimum values) at 2 m above the ground level using CO_2 and environmental parameter (temperature and pressure) measurements averaged at 5-minutes intervals, using 5,000, 10,000, 30,000, and 50,000 particles for all the four steps

Step (run nr.)		Particles number			
		5,000	10,000	30,000	50,000
1	Max	1,250.00	1,140.00	1,130.00	1,140.00
	Min	450.14	450.14	450.14	450.05
2	Max	1,230.00	1,121.46	1,110.00	1,130.00
	Min	453.98	453.98	453.98	453.89
3	Max	1,210.00	1,110.00	1,100.00	1,120.00
	Min	448.51	448.51	448.51	448.42
4	Max	1,200.00	1,100.00	1,090.00	1,100.00
	Min	442.26	442.26	442.26	442.17

Minimum concentration values remained consistent with the measured mean background concentration at the sampling point 1 up to 30,000 particles, then it decreased by a few decimals for 50,000 particles.

Inside the distribution of calculated CO_2 values, the median value is subject to an upward shift to 30,000 particles and then to a downward shift with 50,000 particles for all the steps.

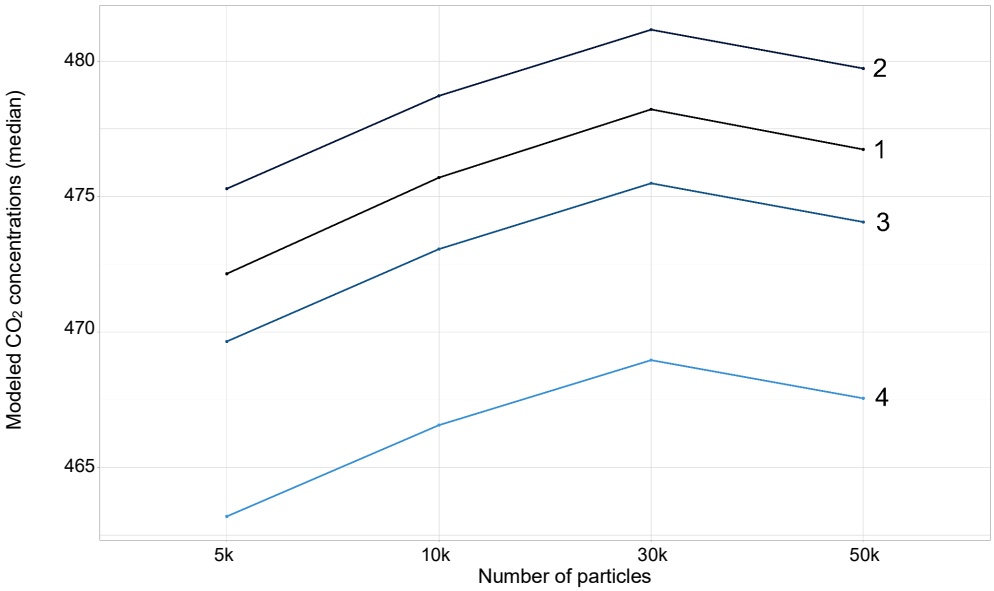

Figure 5. Median modeled CO_2 concentrations of the 16 concentration maps, increasing the number of particles in WindTrax for each step (1–4).

Extending the analysis to the calculated confidence intervals of the estimated CO_2 concentrations, horizontal dispersion maps by WindTrax calculated for the first step are shown in Fig. 6. The same scale of values was used for all the four confidence interval maps, by selecting values from a minimum value of 0 ppm to a maximum value of 290 ppm. It can be observed that by increasing the number of particles included in the simulations, the calculated confidence intervals decreased. Furthermore, as the distance from the source along wind direction increased, the confidence interval decreased.

Pedone et al. (2017) applied the WindTrax model using 2.000, 7.000, and 50.000 particles, obtaining a variability of 20% in CO_2 emission rate. Other authors (Shonkwiler & Ham, 2018; Shaw et al., 2020; Hrad et al., 2021) used the WindTrax model by selecting a number of particles greater than 50,000, mainly for reducing the uncertainty of the model. Studies that selected 50,000 particles adopted smaller distances of sensors from the source i.e. 100–300 m (Hrad et al., 2021), 30 m (Riddick et al., 2022), 0.5 m (Ricco et al., 2021). It should be considered that in studies where sensors are placed close to the source, their number tends to increase. In this study, G-eko units were positioned at 20–40 m from the closer emission source i.e. the bedding inside the livestock building and the manure storage. Hrad et al. (2021) stated that 50,000 particles is the default value to shorten simulation.

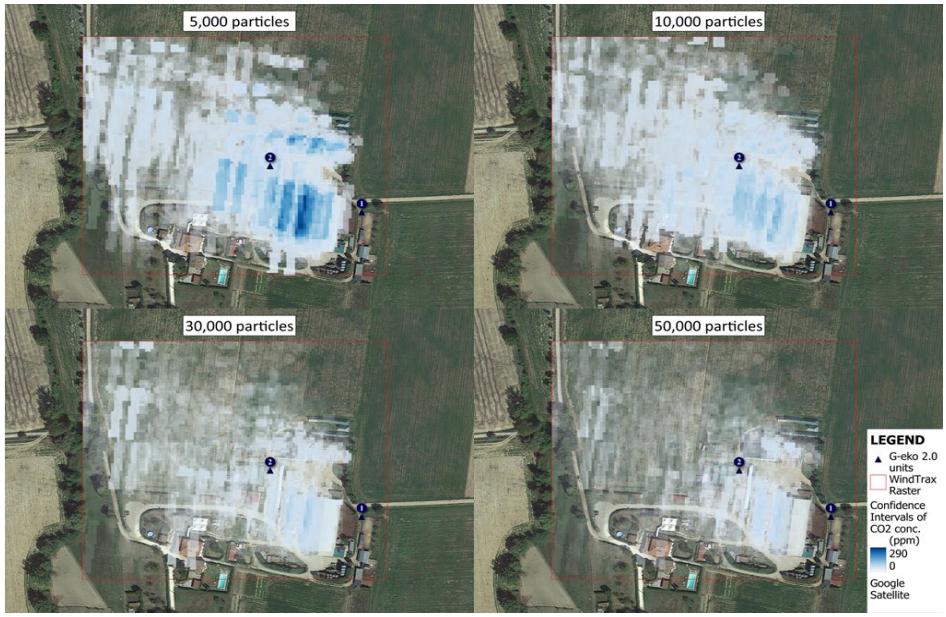

Figure 6. Confidence interval (CI) maps for estimated CO_2 horizontal dispersion at 2 m above ground level modelled with WindTrax simulation using CO_2 measurements averaged at 5-minute intervals. From top left, CI for models computed with 5,000, 10,000, 30,000, and 50,000 particles.

Therefore, simultaneous observation of the concentration maps and the confidence interval maps for the first step (Fig. 3 and 6) showed that the highest values of CO_2 concentration, represented with darker areas, have wider confidence intervals because they are close to the sources. On the other hand, the lowest values represented with lighter areas have smaller confidence intervals because they are further away from the sources. From these considerations, despite the simplicity of applying the bLS approach, the available sensors, type, and positioning have a great impact on atmospheric dispersion simulations.

Table 6. Simulated CO_2 concentration confidence intervals (maximum and minimum values) at 2 m above the ground level using CO_2 and environmental parameter (temperature and pressure) measurements averaged at 5-minutes intervals, using 5,000, 10,000, 30,000, and 50,000 particles for all the four steps

Step (run nr.)		Particles number			
		5,000	10,000	30,000	50,000
1	Max	285.77	144.77	117.00	88.81
	Min	0.00	0.00	0.00	0.16
2	Max	276.62	140.13	113.26	85.96
	Min	0.00	0.00	0.00	0.15
3	Max	274.50	139.06	112.39	85.31
	Min	0.00	0.00	0.00	0.15
4	Max	271.71	137.64	111.25	84.44
	Min	0.00	0.00	0.00	0.15

Table 6 also shows results of the other confidence interval maps, referring to the other steps in terms of maximum and minimum confidence intervals, while Fig. 7 also shows results of the other confidence interval maps, referring to the other steps in terms of median confidence intervals.

For the other steps as well, there is a reduction in the calculated confidence intervals by increasing the number of particles.

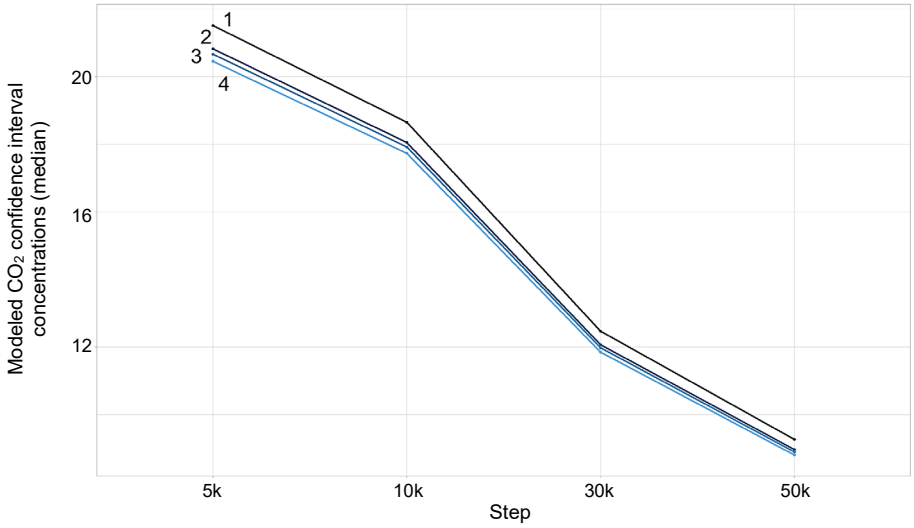

Figure 7. Median modeled CO_2 confidence interval concentrations of the 16 confidence interval concentration maps, increasing the number of particles in WindTrax for each step (1–4).

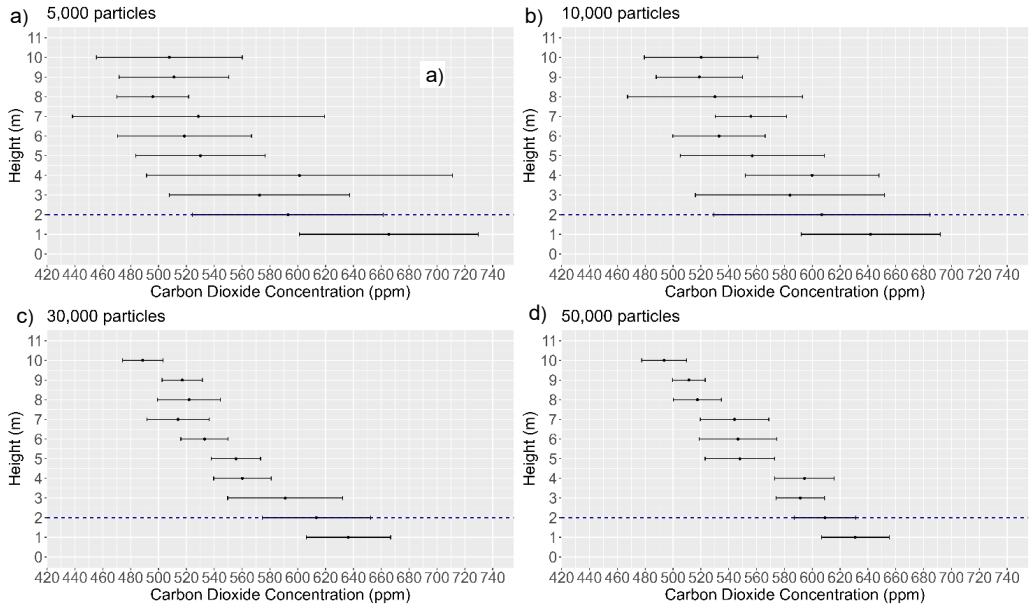

Figure 8. Vertical profile plots of estimated CO_2 concentration confidence intervals in the sampling point 2 of the G–eko 2.0. Simulations were run using 5,000 (a), 10,000 (b), 30,000 (c), and 50,000 (d) particles. Estimations are from heights equal to 1 m a.g.l. to 10 m a.g.l. The dotted blue line indicates the height at which simulations of the horizontal dispersion were carried out.

Additionally, vertical profile plots were calculated with the WindTrax software at the sampling point 2 for observing estimated CO_2 concentrations ± confidence intervals with several numbers of particles at different heights above the ground, i.e. from 0 to 10 m with 1 m intervals. Fig. 8 shows narrower CO_2 confidence intervals as the number

of particles increases. Therefore, what has been observed horizontally with concentration maps and confidence interval maps also occurs vertically with vertical profile plots. Moreover, a better-defined vertical trend in concentrations is observed as the number of particles increases. Again, it is observed that a large number of particles is necessary for a better accuracy in estimating concentrations.

CONCLUSIONS

This study provided relevant insights into the performance of a Lagrangian atmospheric dispersion model for estimating CO_2 emissions from livestock facilities and mapping their dispersion in the surrounding environment.

The results highlight the importance of adapting the measurement protocol to the specific emission sources under investigation. In this case, overall CO_2 emission rates were estimated for three distinct sources: the livestock building, the manure pit, and the slurry tank. To improve source-specific estimates, it is recommended to deploy at least one sensing unit per emission source, along with one additional unit for background concentration measurements. All sensors should be positioned at appropriate distances within a 1 km radius from the sources, in accordance with model guidelines.

With regard to meteorological data processing, the choice of averaging intervals proved critical. Short averaging periods (e.g., 5 minutes) are more susceptible to wind gusts, potentially reducing the reliability of emission rate estimates, particularly under unstable atmospheric conditions. Simulations revealed that increasing the number of particles improved result stability and reduced the width of confidence intervals. Specifically, median concentration values from simulations of horizontal dispersion increased with higher particle counts up to 30,000. Confidence intervals also decreased with greater downwind distance and with increasing number of particles. A particle number of at least 50,000 is recommended to ensure robust model outputs, despite the increased computational demand.

The study also identified several limitations. The limited number of sensing units prevented the estimation of emission rates for individual sources, restricting the analysis of their relative contributions to overall CO_2 emissions. In addition, the proximity of the downwind sensor to the emission sources may have influenced concentration measurements due to local turbulence effects caused by nearby structures. The short duration of the measurement period (20 minutes) and the selected averaging time (5 minutes) may have amplified the influence of wind fluctuations on emission estimates. Furthermore, the use of an anemometer capable of measuring both wind speed and direction-preferably in 2D or 3D-would have improved the characterization of local atmospheric conditions.

Despite these limitations, the WindTrax protocol proved practical and applicable within a livestock farming context, provided that careful attention is paid to sensor placement. Future studies should incorporate a greater number of sensing units and extended monitoring periods to capture diurnal, seasonal, and annual variability in emission rates. Such efforts are essential to improve the bottom-up assessment of greenhouse gas emissions from livestock farming and to support the development of effective mitigation strategies.

ACKNOWLEDGEMENTS. This project was funded by the European Union - Next generation EU for Research Projects of Relevant National Interest (PRIN PNRR 2022) of the Italian Ministry of University and Research (MUR). Project code (CUP): G53D23003800001. 'Emission-controlled intensive livestock housing systems for ecological transition: innovative measuring, mitigating and mapping strategies (EMILI)'.

REFERENCES

Becciolini, V., Conti, L., Rossi, G., Marin, D.B., Merlini, M., Coletti, G., Rossi, U. & Barbari, M. 2023. Real-time measurements of gaseous and particulate emissions from livestock buildings and manure stores with novel UAV-based system. In: *Conference of the Italian Society of Agricultural Engineering*. Cham: Springer International Publishing, pp. 1049–1056.

Becciolini, V., Merlini, M., Massera, E., Bedin Marin, D., Rossi, G. & Barbari, M. 2024a. Performance of a Multi-sensor System for Ground and Aerial Sampling of Pollutants in Livestock Farms. In: *International Mid-Term Conference of the Italian Association of Agricultural Engineering.* Cham: Springer Nature Switzerland, pp. 927–934.

Becciolini, V., Merlini, M., Amantea, R., Verdi, L., Squillace, F., Rossi, G. & Barbari, M. 2024b. Assessment of Carbon Dioxide Measurements from a Prototype Multipollutant Sensor System under Different Environmental Regimes. The 6th *CIGR International Conference 2024*, May 19–23, 2024, Jeju International Convention Center (ICC JEJU), Jeju, Korea.

Burgués, J., Jiménez-Soto, J.M. & Marco, S. 2018. Estimation of the limit of detection in semiconductor gas sensors through linearized calibration models. *Analytica chimica acta* **1013**, 13–25.

Burgués, J. & Marco, S. 2020. Environmental chemical sensing using small drones: A review. *Science of the total environment* **748**, 141172.

Cambra-López, M., Aarnink, A.J., Zhao, Y., Calvet, S. & Torres, A.G. 2010. Airborne particulate matter from livestock production systems: A review of an air pollution problem. *Environmental pollution* **158**(1), 1–17.

Carozzi, M., Loubet, B., Acutis, M., Rana, G. & Ferrara, R.M. 2013. Inverse dispersion modelling highlights the efficiency of slurry injection to reduce ammonia losses by agriculture in the Po Valley (Italy). *Agricultural and Forest Meteorology* **171**, 306–318.

Crenna, B. 2006a. An Introduction to WindTrax. Available at http://www.thunderbeachscientific.com/

Crenna, B. 2006b. Atmospheric data in WindTrax. Available at http://www.thunderbeachscientific.com/

Crenna, B., Flesch, T.K. & Wilson, J.D. 2008. Influence of source-sensor geometry on multi-source emission rate estimates. *Atmospheric Environment* **42**(32), 7373–7383.

Flesch, T.K., Wilson, J.D. & Yee, E. 1995. Backward-time Lagrangian stochastic dispersion models and their application to estimate gaseous emissions. *Journal of Applied Meteorology and Climatology* **34**(6), 1320–1332.

Flesch, T.K. & Wilson, J.D. 2005. Estimating tracer emissions with a backward Lagrangian stochastic technique. *Micrometeorology in agricultural systems* **47**, 513–531.

Genedy, R.A. & Ogejo, J. 2022. Estimating ammonia emitted from manure during storage on a dairy farm. In *2022 ASABE annual international meeting* (p. 1). American Society of Agricultural and Biological Engineers.

Grossi, G., Goglio, P., Vitali, A. & Williams, A.G. 2019. Livestock and climate change: impact of livestock on climate and mitigation strategies. *Animal Frontiers* **9**(1), 69–76.

Hrad, M., Vesenmaier, A., Flandorfer, C., Piringer, M., Stenzel, S. & Huber-Humer, M. 2021. Comparison of forward and backward Lagrangian transport modelling to determine methane emissions from anaerobic digestion facilities. *Atmospheric Environment*: **X**(12), 100131.

IPCC, 2022. Summary for Policymakers. In: Climate Change 2022: Mitigation of Climate Change. Contribution of Working Group III to the Sixth Assessment Report of the Intergovernmental Panel on Climate Change. ISBN 978-92-9169-160-9.

Lin, Z., Liao, W., Yang, Y., Gao, Z., Ma, W., Wang, D., Cao, Y., Li, Y. & Cai, Z. 2015. CH_4 and N_2O emissions from China's beef feedlots with ad libitum and restricted feeding in fall and spring seasons. *Environmental Research* **138**, 391–400.

Martin, C.R., Zeng, N., Karion, A., Dickerson, R.R., Ren, X., Turpie, B.N. & Weber, K.J. 2017. Evaluation and environmental correction of ambient CO 2 measurements from a low-cost NDIR sensor. *Atmospheric measurement techniques* **10**(7), 2383–2395.

Ministero della Salute. 2025. *Banca Dati Nazionale dell'Anagrafe Zootecnica*. Istituto Zooprofilattico Sperimentale dell'Abruzzo e del Molise "G. Caporale". https://www.vetinfo.it/

Mousavi, S.M., Dinan, N.M., Khoshbakht, K., Ansarifard, S., Sonnentag, O. & Naghibi, A. 2025. Determining the influence of meteorological, environmental, and anthropogenic activity variables on the atmospheric CO_2 concentration in the arid and semi-arid regions: A case study in the Middle East. *Atmospheric Research* **319**, 108009.

Pedone, M., Granieri, D., Moretti, R., Fedele, A., Troise, C., Somma, R. & De Natale, G. 2017. Improved quantification of CO_2 emission at Campi Flegrei by combined Lagrangian Stochastic and Eulerian dispersion modelling. *Atmospheric Environment* **170**, 1–11.

R Core Team 2024. R: A language and environment for statistical computing. R Foundation for Statistical Computing, Vienna, Austria. https://www.R-project.org/

Ricco, C.R., Finzi, A., Guido, V., Riva, E., Ferrari, O. & Provolo, G. 2021. Evaluation of ammonia emissions from filtration of digestate used for fertigation. *Journal of Agricultural Engineering* **52**(3), 1187.

Riddick, S.N., Ancona, R., Cheptonui, F., Bell, C.S., Duggan, A., Bennett, K.E. & Zimmerle, D.J. 2022. A cautionary report of calculating methane emissions using low-cost fence-line sensors. *Elementa-Science of the Anthropocene* **10**, 00021.

Ripple, W.J., Smith, P., Haberl, H., Montzka, S.A., McAlpine, C. & Boucher, D.H. 2014. Ruminants, climate change and climate policy. *Nature climate change* **4**(1), 2–5.

RStudio Team 2024. RStudio: Integrated Development for R. RStudio, PBC, Boston, MA URL http://www.rstudio.com/

Shaw, J.T., Allen, G., Pitt, J., Shah, A., Wilde, S., Stamford, L., Fan, Z., Ricketts, H., Williams, P.I., Bateson, P., Barker, P., Purvis, R., Lowry, D., Fisher, R., France, J., Coleman, M., Lewis, A.C., Risk, D.A. & Ward, R.S. 2020. Methane flux from flowback operations at a shale gas site. *Journal of the Air & Waste Management Association* **70**(12), 1324–1339.

Shonkwiler, K.B. & Ham, J.M. 2018. Ammonia emissions from a beef feedlot: Comparison of inverse modeling techniques using long-path and point measurements of fenceline NH_3. *Agricultural and Forest Meteorology* **258**, 29–42.

Tagliaferri, F., Invernizzi, M., Capra, F. & Sironi, S. 2023. Validation study of WindTrax reverse dispersion model coupled with a sensitivity analysis of model-specific settings. *Environmental research* **222**, 115401.

Tagliaferri, F., Invernizzi, M., Sironi, S. & Capelli, L. 2020. Influence of modelling choices on the results of landfill odour dispersion. *Detritus* **12**, 92–99.

Wickham, H. 2016. ggplot2: Elegant Graphics for Data Analysis. Springer-Verlag New York. ISBN 978-3-319-24277-4, https://ggplot2.tidyverse.org

Yang, W., Zhu, A., Zhang, J., Zhang, X. & Che, W. 2016. Assessing the backward Lagrangian stochastic model for determining ammonia emissions using a synthetic source. *Agricultural and Forest Meteorology* **216**, 13–19.